

This article was downloaded by:

On: 25 January 2011

Access details: *Access Details: Free Access*

Publisher *Taylor & Francis*

Informa Ltd Registered in England and Wales Registered Number: 1072954 Registered office: Mortimer House, 37-41 Mortimer Street, London W1T 3JH, UK



Liquid Crystals

Publication details, including instructions for authors and subscription information:

<http://www.informaworld.com/smpp/title~content=t713926090>

Morphology and electro-optical properties of nematic liquid crystal/Aerosil® nanoparticle composites

Sabrina Mormile^a; Giovanni De Filpo^a; Giuseppe Chidichimo^a; Fiore Pasquale Nicoletta^b

^a Dipartimento di Chimica, Università della Calabria, Arcavacata di Rende (CS), Italy ^b Dipartimento di Scienze Farmaceutiche, Università della Calabria, Arcavacata di Rende (CS), Italy

To cite this Article Mormile, Sabrina , De Filpo, Giovanni , Chidichimo, Giuseppe and Nicoletta, Fiore Pasquale(2008) 'Morphology and electro-optical properties of nematic liquid crystal/Aerosil® nanoparticle composites', *Liquid Crystals*, 35: 9, 1095 – 1100

To link to this Article: DOI: 10.1080/02678290802376115

URL: <http://dx.doi.org/10.1080/02678290802376115>

PLEASE SCROLL DOWN FOR ARTICLE

Full terms and conditions of use: <http://www.informaworld.com/terms-and-conditions-of-access.pdf>

This article may be used for research, teaching and private study purposes. Any substantial or systematic reproduction, re-distribution, re-selling, loan or sub-licensing, systematic supply or distribution in any form to anyone is expressly forbidden.

The publisher does not give any warranty express or implied or make any representation that the contents will be complete or accurate or up to date. The accuracy of any instructions, formulae and drug doses should be independently verified with primary sources. The publisher shall not be liable for any loss, actions, claims, proceedings, demand or costs or damages whatsoever or howsoever caused arising directly or indirectly in connection with or arising out of the use of this material.

Morphology and electro-optical properties of nematic liquid crystal/Aerosil® nanoparticle composites

Sabrina Mormile^a, Giovanni De Filpo^{a*}, Giuseppe Chidichimo^a and Fiore Pasquale Nicoletta^b

^aDipartimento di Chimica, Università della Calabria, Arcavacata di Rende (CS), Italy; ^bDipartimento di Scienze Farmaceutiche, Università della Calabria, Arcavacata di Rende (CS), Italy

(Received 5 May 2008; final form 29 July 2008)

Liquid crystalline materials play an important role in the synthesis of nanoparticles of well-defined shape and size; at the same time nanoparticles dispersed in liquid crystals allow investigation of defect formation in liquid crystal suspensions and enhance the light scattering properties of nematic cells. The morphology and the electro-optical properties were investigated of thin films of nematic liquid crystal/Aerosil® nanoparticle composites, in which the Aerosil® nanoparticles are interconnected by free radical polymerisation. The prepared cells are characterised by high contrast ratios, large switching electric fields, but very fast relaxation times. In addition, memory effects were observed in the samples, since Aerosil® particles tended to generate local defects in the liquid crystal after the first switching run.

Keywords: nanoparticle composites; Aerosil®; light scattering

1. Introduction

Nanoparticles and liquid crystals represent an example of an interesting connection between two different research fields, both of which involve the enhancement of the performance of their respective products (1). In fact, new synthetic procedures have been designed for the preparation of nanostructures with well-defined shape and size, employing liquid crystalline templates that are able to match both order and mobility at a nanoscale level (2–7). At the same time there are several fascinating examples of liquid crystals that interact with nanoparticles dispersed within them. In general, liquid crystal droplets are dispersed in a polymer matrix or small amounts of polymer are “jellified” in a liquid crystal (8). Due to the high surface to volume ratio, the polymer influences the surrounding liquid crystal orientational order, which is the result of competition among polymer wall anchoring and temperature and external field effects (9, 10). Minimisation of the elastic free energy leads to the formation of anisotropic colloidal structures (11) and various types of topological defects (12).

Nanoparticles dispersed in liquid crystals give rise to devices affected by memory effects, i.e. the original OFF state transmittance is not recovered after removal of the field (13–15). The given explanation is that the liquid crystal reorientation causes a reorganisation of the initial random arrangement of nanoparticles, which then stabilises the oriented state or a state more ordered than the initial one (16, 17).

The magnitude of the memory effect is related to the number of available surface groups that can form bonds with liquid crystal molecules (18).

Recently, Aerosil® nanoparticles dispersed in nematic (including chiral mesophase) liquid crystals have been extensively studied (19–22) for their electro-optical properties and memory effects. Their intense light scattering in the OFF state is due to the large number of orientational defects generated by the dispersed particles. The application of an external field causes the reorientation of nematic directors and the transparency of films. In this paper, we report an investigation of the morphology and electro-optical properties of thin films of nematic liquid crystal/Aerosil® nanoparticles composites, in which the Aerosil® nanoparticles are interconnected to form a network by free radical polymerisation. In addition, the memory effect has been quantified and related to the physico-chemical properties and concentration of the particles.

2. Experimental

Materials

The liquid crystal used in this work was E49 (Merck, Germany), which is a eutectic mixture of 4-alkylcyano-biphenyls, characterised by a positive dielectric anisotropy ($\Delta\epsilon=17$) and by the following phase sequence: smectic (-20°C) \rightarrow nematic (100°C) \rightarrow isotropic. Aerosil® nanoparticles were pyrogenic silicon dioxide type R711 and R7200 (Degussa, Germany),

*Corresponding author. Email: defilpo@unical.it

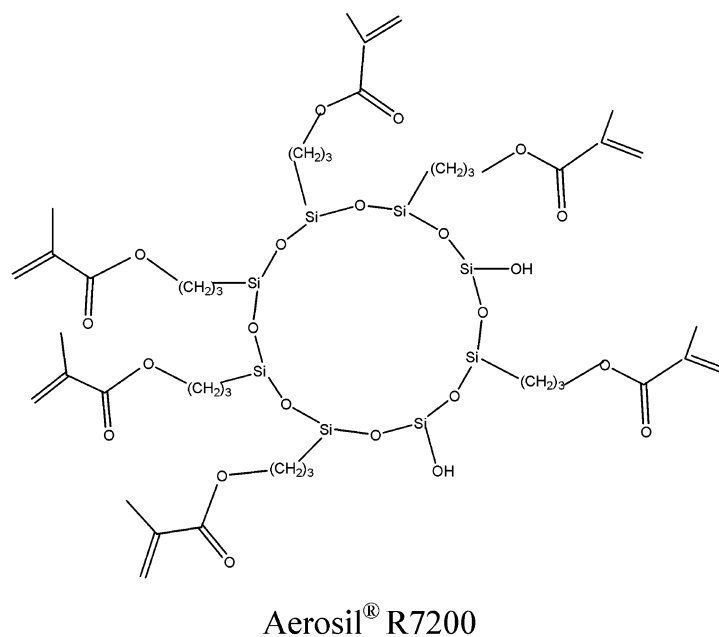
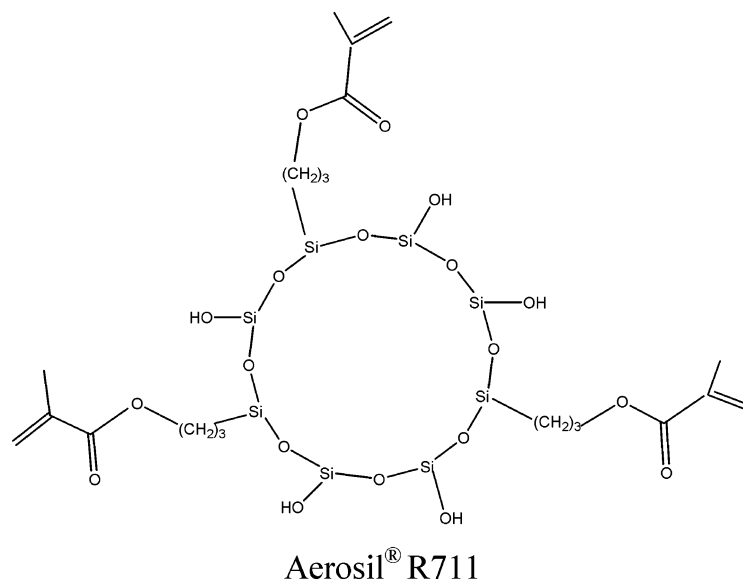


Figure 1. Schematic display of the primary particle aggregates, which form (a) Aerosil® R711 and (b) Aerosil® R7200.

which have surfaces functionalised with methacrylic groups, as shown in Figure 1, and differ in the percentage of methacrylic surface coverage (23). Both Aerosil® primary particles have a size of the order of 12 nm and the residual Si–OH groups form aggregates among different primary particles with a very large specific surface area ($\approx 150 \text{ m}^2 \text{ g}^{-1}$) and different packing density (60 g l^{-1} for R711 and 230 g l^{-1} for R7200, respectively), which is not derived from porosity (24). Both nanoparticles are derived from Aerosil® 200 nanoparticles, which do not contain carbon atoms. As

a consequence, we checked the difference between R711 and R7200 surface coverages by a simple elemental analysis (CHNS). We found the following C (wt%) contents: $C_{R711}:C_{R7200}=5.59:7.50 \approx 2:3$, i.e. R7200 aggregates are characterised by a larger methacrylic surface coverage, as shown in Figure 1.

Samples

Two different approaches were followed for sample preparation. The first one involved the preparation of

matrixes by polymerisation of silica nanospheres followed by the absorption of liquid crystal by capillary suction. The second protocol consisted of the preparation of nanoparticle dispersions in the liquid crystal and the subsequent polymerisation of nanospheres. Both procedures lead to porous three-dimensional (3D) structures within which liquid crystal is dispersed.

First procedure

In order to achieve uniform polymerisation, nanospheres were homogeneously dispersed in a solvent containing UV initiator (2 wt% respect to silica of 2,2'-dimethoxy-1,2-diphenylethan-1-one, Irgacure 65, Ciba). Different solvents were used (diethyl ether, octanol, and mixtures of butanol, acetylacetone and Triton X100 in different weight percentages with respect to silica). The best results were obtained with octanol (probably due to its high boiling point, b.p.=188°C, see subsequent discussion) in the following weight ratios R711:octanol=1:4 and R7200:octanol=1:2. A small amount of the suspension was cast on conductive glass substrates covered with a thin film of indium–tin oxide and a second conductive substrate was placed on the suspension to form a cell. Glass spheres were added in order to ensure a cell gap of 37µm. Finally, the cells were UV irradiated to induce crosslinking among the silica particles. UV light power, irradiation time and solvent evaporation rate are important parameters that can influence the final morphology. The best polymerisation conditions were: low UV powers (around 5 mW cm⁻²) and long irradiation times (more than 1 h, average supplied energy 20 J cm⁻²). The long UV irradiation time caused an increase in the sample temperature and in the solvent evaporation rate, which lead to a lack of film homogeneity. Several solvent evaporation trials were followed including: evaporation at room temperature, evaporation under vacuum, low-temperature evaporation and evaporation in a solvent-saturated atmosphere. The best morphologies were obtained with the latter evaporation conditions with octanol as solvent.

Second procedure

According to this procedure, silica nanospheres and initiator were dispersed in liquid crystal by using a small amount of acetone, which was then evaporated. The silica to liquid crystal weight ratios were varied from 5 to 25 wt%. This procedure required complete solvent evaporation before the second conductive substrate is added. Then samples were UV irradiated using the same conditions reported for the first

procedure. In fact, the application of larger UV powers caused cracks in the film morphology, whereas lower exposure times did not allow a complete polymerisation of the nanoparticles.

Measurements

Sample morphologies were investigated by polarising optical and scanning electron microscopy (POM and SEM, respectively). POM analysis was carried from the cell top side. SEM was performed on cross-sections of films, cut after immersion in liquid nitrogen, left under vacuum for several hours in order to extract the liquid crystal (in the case of samples prepared according to the second procedure), gold coated and finally examined by a Leica LEO 420 scanning electron microscope. The electro-optical properties of samples were measured using a previously reported optical setup (25). The intensity of the incident light measured through an empty cell was assumed to be full-scale intensity. The ON and OFF response times, τ_{ON} and τ_{OFF} , defined, respectively, as the time required for the transmittance to change from 10% to 90% of its maximum and to decrease from 90% to 10% of the optical response after the external field is removed, were determined by monitoring the drive signal ($\nu=1$ kHz, $E_{pp}=20$ V µm⁻¹) and the response of the photodiode using a digital storage oscilloscope.

3. Results and discussion

The use of Aerosil® R711 and Aerosil® R7200 did not result in any particular difference in the morphology of the composites obtained, even though the first type of structure was more fragile, probably due to the lower number of methacrylic groups present on the surfaces of silica aggregates. As a consequence, R711 samples did not give good electro-optical devices and their electro-optical response was not investigated. Morphology behaviour was very similar for both the procedures followed for the preparation of samples. In fact, both POM and SEM highlighted that the use of octanol as solvent and its evaporation in a saturated solvent atmosphere allow the preparation of structures, according to the first procedure, which were not fragmented and rather dense at nanoscale level, as shown in the SEM picture of Figure 2. In contrast, the use of other solvents and evaporation conditions led to large fragmentations on a scale of 100 µm, as shown by the POM picture in Figure 3. At larger magnifications it is possible to observe that the morphology of these samples is again rather dense and to hypothesise that the fragmentation is due to the internal stresses originating inside the samples.

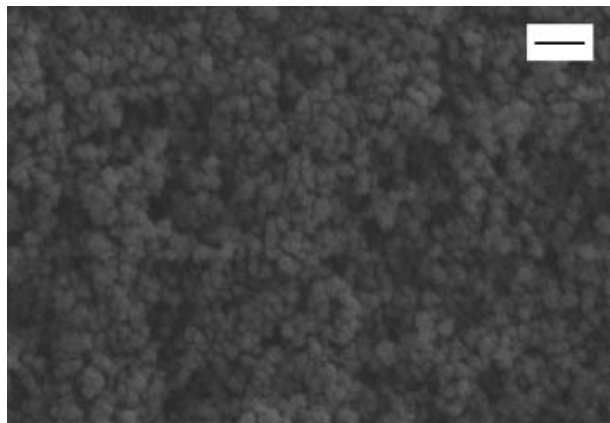


Figure 2. SEM picture of the typical morphology exhibited by samples prepared in an octanol-saturated atmosphere. The bar is equal to 50 nm.

As shown in Figure 2, samples prepared with slow evaporation rates are characterised by a good silica nanoparticle distribution and they are inserted among empty crevices in the case of the first preparation procedure and among liquid crystal-filled voids for the second preparation procedure. Nevertheless, we were not able to induce absorption of liquid crystal (by capillary suction) in an adequate manner in the samples prepared by the first procedure. In contrast, good results were obtained with the single-step procedure (polymerisation of liquid crystal and nanoparticles mixtures). Films prepared with a higher particle percentage (30 wt% and 35 wt%) are characterised by a very dense structure, with no electro-optical switching due to the very small domain size. Samples obtained with a lower silica content (from 10 wt% to 25 wt%) are characterised by an average interstice size that allows the transition from the opaque to the transparent state by the application of a suitable electric field

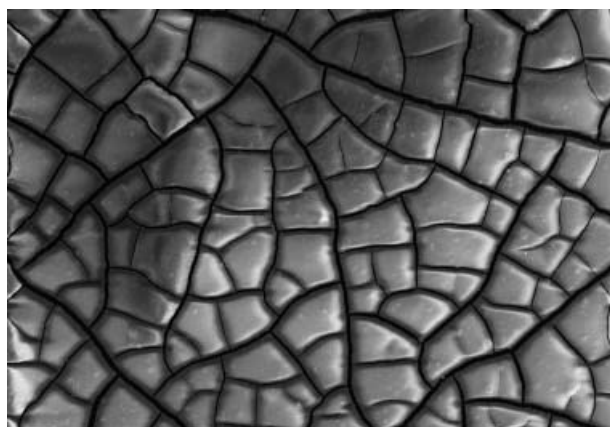


Figure 3. Lack of homogeneity in the morphology of samples prepared according to the first procedure. Picture size is $850 \mu\text{m} \times 600 \mu\text{m}$.

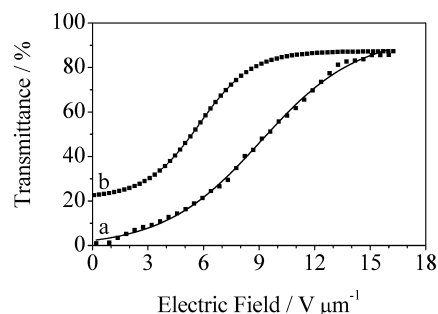


Figure 4. Electric field-dependent transmittance of a nematic liquid crystal/Aerosil® R7200 composite: (a) first run; (b) subsequent runs. Liquid crystal content was 85 wt%. Measurements were performed at 25°C .

($E_{90\%} = 12 \text{ V } \mu\text{m}^{-1}$), as shown in Figure 4(a). In fact, the switching fields are affected by interfacial interaction between liquid crystal and nanoparticles and, consequently by their relative amounts in samples: the larger the nanoparticle concentration, the smaller the voids, and consequently the higher the switching fields. In contrast, very low silica concentrations (less than 10 wt%) did not provide well cross-linked networks, the samples being too fluid.

The initial OFF state transmittances of samples decreased with increasing content of Aerosil® particles because the increase of defects generated in liquid crystal and the mismatch of the refractive indices between Aerosil® particles and liquid crystal phase ($T < 1\%$). The initial OFF state transmittance value was lower than the value of the OFF state transmittance obtained after the first run (Figure 4(b)), revealing the presence of a memory effect. The values of the OFF state transmittance after the following runs were equal to second one and stable over long time at room temperature.

It is known that memory effects affect the light scattering properties of nematic liquid crystal/nanoparticles dispersions due to the generation of orientation defects after the application of an external field. This effect was explained for silica nanoparticles in a liquid crystal matrix as a reorganisation of the initial random structure of the Aerosil® network due to the nematic director reorientation under the applied electric field. As a consequence, the memory effect could simply be the result of network rearrangements in the presence of the field, i.e. it could simply be related to the non-annealing of strains. In the case of a polymerised silica network we cannot exclude that the memory effect is related also to a modification of nanoparticle surfaces under the action of oriented liquid crystal in a similar manner to the memory effect observed in polymer-dispersed liquid crystals after a charge process (26). In order to better clarify these

hypotheses, we measured the changes in the residual transmittance after the application of the field as a function of temperature. We observed that samples kept their residual OFF state transmittance up to the clearing point of the liquid crystal ($T=100^{\circ}\text{C}$). Above this temperature we observed a larger reduction of the residual transmittance, but it did not completely disappear. We cycled the experiment several times, but there were no significant changes in the residual transmittance. This experiment allows us to confirm that both hypotheses are valid, i.e. the residual transmittance can be attributed both to a residual orientation of liquid crystal molecules at the nanoparticle surface (which is lost at the nematic–isotropic transition temperature) and to a network rearrangement in the presence of the field (which is kept even at high temperatures). To describe the strength of memory effects, it is convenient to define a memory percentage, M , as:

$$M = \frac{T_r - T_i}{T_f - T_i} \times 100, \quad (1)$$

where T_i , T_f and T_r are, respectively, the initial OFF state transmittance, the final ON state transmittance and the residual OFF state transmittance (i.e. after the external field removal). We found that M increases with nanoparticle content and ranges from 50% to 8% if the silica concentration increases from 10 to 25% (see Figure 5).

From Figure 4(b), it is possible to observe a severe change in the shape of the electro-optical curve. In particular, the switching field is strongly reduced from 12 to $8\text{ V}\mu\text{m}^{-1}$ and the slope of transmittance versus field increases after the first

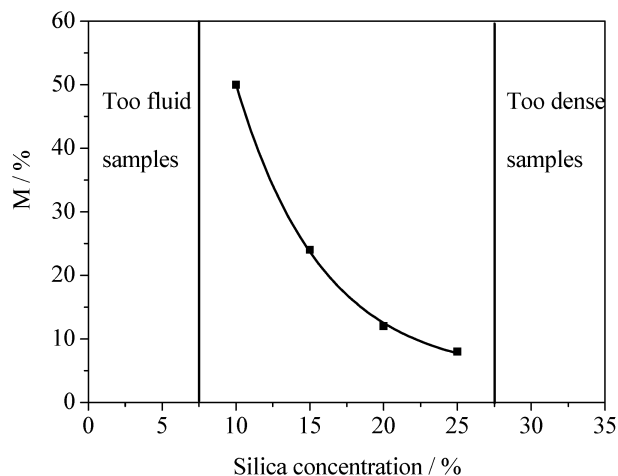


Figure 5. Behaviour of memory percentage, M , as a function of silica concentration. Measurements were performed at 25°C .

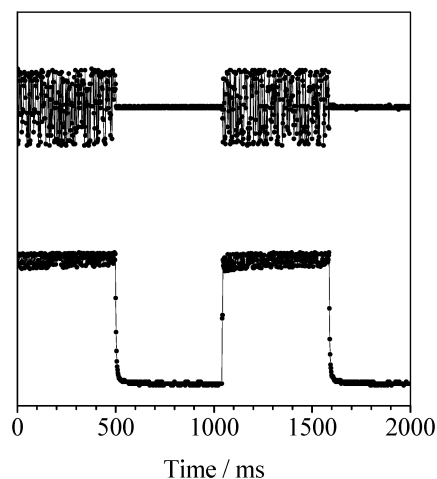


Figure 6. Typical electro-optical response of a nematic liquid crystal/Aerosil® R7200 composite. Liquid crystal content was 75 wt%. Measurements were performed at 25°C .

run, i.e. samples are characterised by a sharper threshold. The electro-optical response is rather fast, as shown in Figure 6. The ON response is of the order of a few milliseconds (2–4 ms), whereas the OFF response time is of the order of some tens of milliseconds (14–30 ms). Such values are in agreement with those reported in polymer-dispersed liquid crystals with a reverse morphology (polymer ball morphology) (8).

4. Conclusions

We have successfully prepared electro-optical devices formed by the polymerisation of a silica nanoparticle/liquid crystal dispersion. Films prepared with Aerosil® R7200 were free from defects and characterised by a homogeneous distribution of nanoparticles in the liquid crystal phase after choosing the best conditions among UV polymerisation powers, irradiation times and solvent evaporation rates. The composites were able to undergo an electro-optical transition from a highly scattering OFF state to a transparent ON state by application of electric fields of about $10\text{ V}\mu\text{m}^{-1}$. The best results were obtained by using Aerosil® R7200 silica nanoparticles, which contain a larger methacrylic group number per primary particle. They gave more dense and less fragile networks than those obtained by using Aerosil® R711 nanoparticles. Very soft solvent evaporation conditions gave the best results, both in morphology and electro-optical performances. The use of such samples could be interesting both from a theoretical and experimental point of view to study the order of liquid crystal in restricted geometries

characterised by a uniform size and well-defined refractive index.

Acknowledgments

MIUR is acknowledged for financial supports (EX-60% and PRIN).

References

- (1) Hegmann T.; Qi H.; Marx V.M. *J. Inorg. Organometallic Polym. Mater.* **2007**, *17*, 483–508.
- (2) Gole A.; Murphy C.J. *Chem. Mater.* **2004**, *16*, 3633–3640.
- (3) Thomas A.; Schlaad H.; Smarly B.; Antonietti M. *Langmuir* **2003**, *19*, 4455–4459.
- (4) Karanikolos G.N.; Alexandridis P.; Mallory R.; Petrou A.; Mountziaris T.J. *Nanotechnology* **2005**, *16*, 2372–2380.
- (5) Dobbs W.; Suissa J.-M.; Douce L.; Welter R. *Angew. Chem., Int. Ed.* **2006**, *45*, 4179–4182.
- (6) Mougous J.; Baker R.; Patrick D.L. *Phys. Rev. Lett.* **2000**, *84*, 2742–2745.
- (7) Dierking I.; Scalia G.; Morales P.; Leclere D. *Adv. Mater.* **2004**, *16*, 865–869.
- (8) Drzaic P.S. *Liquid Crystal Dispersions*; World Scientific: Singapore, 1995.
- (9) Crawford G.P.; Zumer S. *Liquid Crystals in Complex Geometries Formed by Polymer and Porous Networks*; Taylor & Francis: London, 1996.
- (10) Chiccoli C.; Pasini P.; Skacej G.; Zannoni C.; Zumer S. *Phys. Rev. E* **2003**, *67*, 010701, 1–4.
- (11) Poulin P.; Stark H.; Lubensky T.C.; Weitz D.A. *Science* **1997**, *275*, 1770–1773.
- (12) Poulin P.; Weitz D.A. *Phys. Rev. E* **1998**, *57*, 626–637.
- (13) Levy D.; Serna C.J.; Oton J.M. *Mater. Lett.* **1998**, *10*, 470–476.
- (14) Oton J.M.; Serrano A.; Serna C.J.; Levy D. *Liq. Cryst.* **1991**, *10*, 733–739.
- (15) Kreuzer M.; Tschudi T.; Eidenschink R. *Mol. Cryst. Liq. Cryst.* **1992**, *223*, 219–227.
- (16) Eidenschink R.; de Jeu W.H. *Electron. Lett.* **1991**, *27*, 1195–1196.
- (17) Bellini T.; Buscaglia M.; Chiccoli C.; Mantegazza F.; Pasini P.; Zannoni C. *Phys. Rev. Lett.* **2002**, *88*, 245506, 1–4.
- (18) Glushchenko A.; Kresse H.; Reshetnyak V.; Reznikov Y.; Yaroshchuk O. *Liq. Cryst.* **1997**, *23*, 241–246.
- (19) Sikharulidze D. *Appl. Phys. Lett.* **2005**, *86*, 033507, 1–3.
- (20) Dolgov L.O.; Yaroshchuk O.V. *Colloid Polym. Sci.* **2004**, *282*, 1403–1408.
- (21) Dioriojr N.J.; Fish M.R.; West J.W. *Liq. Cryst.* **2002**, *29*, 589–596.
- (22) Li B.; Huang H.; Ding X.; Li W.; Wang L.; Cao H.; Yang H. *Liq. Cryst.* **2008**, *35*, 49–54.
- (23) Degussa Corp, Silica Division *Aerosils*; Frankfurt am Main, 2000.
- (24) Michael G.; Ferch H. *Technical Bulletin on Pigments* No. 11, Degussa Corp, 2004.
- (25) Chidichimo G.; Huang Z.; Caruso C.; De Filpo G.; Nicoletta F.P. *Mol. Cryst. Liq. Cryst. Sci. Technol. A* **1997**, *299*, 379–387.
- (26) Cupelli D.; Macchione M.; Nicoletta F.P.; De Filpo G.; Chidichimo G. *Liq. Cryst.* **2001**, *28*, 287–290.